Robotica (2001) volume 19, pp. 439–449. Printed in the United Kingdom © 2001 Cambridge University Press

On dynamic stability of manipulators mounted on mobile platforms

R.F. Abo-Shanab and N. Sepehri

Department of Mechanical and Industrial Engineering, The University of Manitoba, Winnipeg, Manitoba (Canada) R3T-5V6

(Received in Final Form: October 24, 2000)

SUMMARY

This paper presents the development of a model which can adequately simulate the dynamic stability of manipulators mounted on moveable platforms. The model takes into account the dynamics of the base that can potentially rock back-and-forth. Particularly, the model predicts the changes in the velocities of the manipulator links and the base due to impact with the ground. The application of the study is directed at industrial machines that carry human-operated hydraulic manipulators. The model is therefore used to simulate for the first time, planar movements of'a Caterpillar 215B excavator-based log-loader. The results clearly show the effect of the manipulator movement on turning the base over. The results also show that by proper manipulation of the arms, one can achieve a stable condition and even reverse the 'tipover' situation in such machines.

KEYWORDS: Mobile platforms; Dynamic stability; Manipulators; Industrial machines.

1. INTRODUCTION

The development of automated systems for the operation of heavy-duty manipulator-like hydraulic machines, such as log-loaders, has recently received increased attention. The environments in which these machines operate are unstructured and potentially hazardous. The operator must remain constantly alert in order to accomplish the work efficiently and, at the same time protect his/her safety and that of others. Current research effort has been to develop means for converting these machines into teleoperated control systems.[1] One issue in the computer control of such machines, is the ability to maintain stability. A heavy-duty mobile manipulator while carrying a load, experiencing a force, or operating on uneven terrain needs to maintain its balance.

Early work on stability of mobile vehicles was only concerned with the static stability and gait generation of slow moving legged machines (see the work by Messuri and Klein[2] and the references listed therein). These methods could deal with cases where the only destabilizing load is due to the gravitational force. In a moving-base manipulator, however, a large portion of destabilizing forces and moments could be due to the inertial or external loads arising from maneuvering the implement. Dubowsky and Vance[3] proposed a time optimal motion planning strategy for manipulators that are mounted on mobile platforms. The goal was to allow the manipulators to perform tasks quickly without generating dynamic forces and moments that cause the system to overturn. The method, however, did not attempt to study the tipover case or to develop a measure of stability. Sugano *et al.*[4] and Huang *et al.*[5] employed the ZMP (Zero Moment Point) concept and constructed a quantitative criterion for stability measure of manipulators mounted on vehicles. In their work, the manipulator, including the vehicle and the payload, was considered to be a system of particles moving on only rigid horizontal floors. ZMP concept is a moment-based approach and therefore does not include the effect of the walking height in the stability analysis. Papadopoulos and Rey[6,7] proposed a Force-Angle measure of tipover stability margin, which has a simple graphical interpretation and is easy to compute. The 'Force-Angle' method, however, predicts the same stability measure for all locations of the center of gravity that lie in a line passing through the edge of potential overturning. Ghasempoor and Sepehri[8] discussed that the energy stability method by Messuri and Klein[2] is the only measure of stability that can quantitatively show the effects of top-heaviness and sloping ground. They then extended this method to also reflect the effect of forces and moments arising from the manipulation of the implement. The significance of this extension is that it can be used as an off-line tool to provide the designer with an inexpensive and fast method that helps to maintain the stability of mobile manipulators. The extension, however, did not consider the dynamic situation, i.e., tipover of the entire machine during an unstable stance. Moreover, depending upon the subsequent states of the implement motion, the entire machine may rock back-and-forth, a phenomenon that cannot be characterized by any of the previously developed methods including the ones described above.

The goal of the work reported in this paper is to develop a model that contains enough features to yield the behavioral information on dynamic stability of heavy-duty hydraulic machines that carry manipulators. The model is built upon the simulation model, developed previously by Sepehri *et al.*,[1,9] for a Caterpillar 215B log-loader machine (see Fig. 1) and includes models to accurately incorporate the dynamics of the rocking base in such machines. These machines incorporate many aspects of typical robotic systems and are the basis for most heavy-duty hydraulic machines. Thus, the analyses and development reported in

https://doi.org/10.1017/S0263574701003356 Published online by Cambridge University Press

Fig. 1. Typical mobile manipulator; a Caterpillar 215B excavator-based log-loader.

this paper can be applied to other similar mobile robotic systems or heavy-duty mobile manipulators.

The organization of this paper is as follows. Section 2 describes the candidate machine, a Caterpillar 215 based log-loader. Then the dynamic model of the machine during a planar motion is outlined in Section 3. This includes modelling of the linkages, collision of the base with the ground during the rocking motion, as well as the hydraulic driving unit. Particularly, the mathematical model of the manipulator collision with the environment by Zheng and Hemami[11] has been adapted to model the impact of the base with the ground. This present model requires the edge of instability to be modeled as a free joint.

In order to facilitate the application of conventional Lagrange-Euler method of modeling serial-link robot arms, the free joint here is modeled by adding two virtual links with two prismatic joints. Section 4 describes the computational algorithm. Section 5 demonstrates typical simulation results. It is shown that by proper manipulation of the links, one can achieve a stable condition and can even reverse the tipover situation. The results are also shown to be in agreement with the results obtained from the energy stability method by Ghasempoor and Sepehri.[8] Conclusions are finally given in Section 6.

The novelty in this work, which is believed to be a further contribution to the stability analysis of mobile manipulators, is that the model considers both the tipover of the base and the impact with the ground. The resulting model will therefore, provide simulation capabilities to facilitate design of suitable tipover prevention schemes.

2. MACHINE DESCRIPTION

The Caterpillar 215B based log-loader (see Fig. 1) is a mobile three degree of freedom manipulator with an additional moveable implement. The implement is a grapple for holding and handling objects such as trees. The whole machine can move forward or backward on its tracked undercarriage. The upper structure of the machine rotates on the carriage by a ‘swing’ hydraulic motor through a gear train. ‘Boom’ and ‘stick’ are the two other links, which together with the ‘swing’, serve to position the implement. Boom and stick are operated through hydraulic cylinders. The cylinders and the swing motor are activated by means of pressure and flow through the main valves. Modulation of the oil flow in the main valves is presently controlled by the pilot oil pressure through manually operated pilot control valves. This heavy-duty machine can be considered as a manipulator mounted on a mobile platform.

3. OUTLINE OF THE MODELING

In this section, the equations describing the dynamic stability of the log-loader are derived. Here, we assume that the swing is locked thus, the movement of the implement is limited to a planar motion. The treatment of the three-dimensional movement of the end-effector is a straightforward extension of the analysis presented here. Furthermore, it is assumed that the contact ground is solid and the impact of the base with the ground is plastic. With reference to Fig. 2. the system to be modeled can be characterized by three distinct phases:

Phase 1: The platform is stable and thus not moving (see Fig. 2a). This refers to a case whereby the manipulator movement does not affect the stability and the model consists of only dynamic equations as that of a two-link manipulator.

Phase 2: The base is turning over the rear edge or the front edge. This situation is schematically shown in Fig. 2b. This is the case whereby the forces and moments arising from the implement movements can no longer be sustained by the vehicle without overturning. Assuming that the friction between the ground and the machine base is sufficient to only allow the rotation, the machine can be modeled as a three-link manipulator.

Phase 3: The base rocks back-and-forth. For example, with reference to Fig. 2c, the machine rolls over edge A towards a stable position. At the point of contact, the system suffers an impulsive force, which causes discontinuities in joint angular velocities of all links, including the base. The states of the machine and the impulsive forces arising at the instant of impact will determine the subsequent states after the impact.

First the dynamic models for first and second phases are briefly outlined. Then, the dynamic model for the third phase is derived in detail.

3.1. Dynamic model for cases of no impact

As described in the previous section, the first and second phases have no impact with the ground. So, the first phase can be modeled as a two-link serial manipulator. The second phase can be modeled as a three-link serial robot manipulator assuming that there is a hypothetical joint at the point of contact between the ground and the base. The dynamic equations describing the above two phases are simply

https://doi.org/10.1017/S0263574701003356 Published online by Cambridge University Press

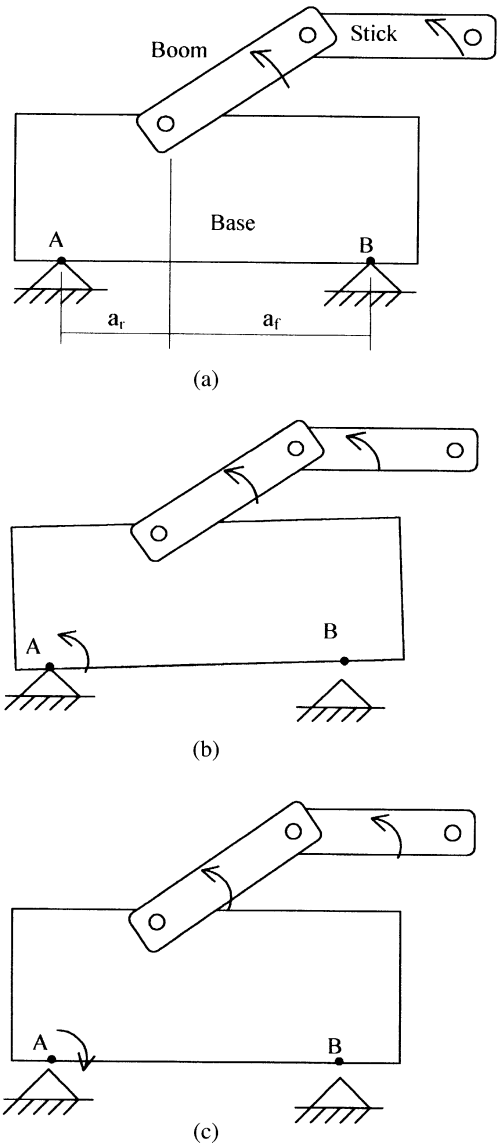

Fig. 2. Different phases of the base in a mobile manipulator: (a) base is stable; (b) base is turning over the rear edge; (c) just before the impact with the ground.

derived based on Lagrange equation as follows (see reference [11] for details):

$$\tau(t)=\mathbf{D(q)}\ddot{\mathbf{q}}+\mathbf{C(q,}\dot{\mathbf{q}}\mathbf{)}+\mathbf{H(q)} \tag{1}$$

where $\tau(t)=\{\tau_1,\ \tau_2, \ldots, \tau_n\}^T$ is the generalized force vector applied at joints $i=1, 2, \ldots, n$. $\mathbf{D(q)}$ is an $n \times n$ inertial acceleration-related symmetric matrix whose elements are:

$$D_{ij}=Trace\left\{\Delta_i\left[\sum_{p=j}^{n}\mathbf{T}_p\mathbf{J}_p\mathbf{T}_p^T\right]\Delta_j^T\right\} \qquad (j\geq i)$$

$$D_{ji}=D_{ij} \tag{2}$$

$\mathbf{C}(\mathbf{q},\dot{\mathbf{q}})=\{c_1,\ c_2, \ldots, \ c_n\}^T$ denotes nonlinear coriolis and centritugal forces; its elements are:

$$c_i=\sum_{j=1}^{n}\sum_{i=1}^{n}c_{ijk}\dot{q}_j\dot{q}_k \tag{3}$$

where

$$c_{ijk}=Trace\left\{\Delta_i\left[\sum_{p=j}^{n}\mathbf{T}_p\mathbf{J}_p\mathbf{T}_p^T\right]\Delta_k^T\Delta_j^T\right\} \qquad (j\geq i,\ k)$$

$$c_{ikj}=c_{ijk}\ \&\ c_{kji}=-c_{ijk} \qquad (j\leq i,\ k)$$

and

$$\mathbf{J}_p=\begin{bmatrix}\mathbf{I}_p+m_p\mathbf{r}_p\mathbf{r}_p^T & m_p\mathbf{r}_p\\ m_p\mathbf{r}_p^T & m_p\end{bmatrix}$$

Finally $\mathbf{H(q)}=\{h_1,\ h_2, \ldots, \ h_n\}^T$ in (1) is the gravitational force vector whose elements are:

$$h_i=-(\mathbf{g}^T;\ 0)\Delta_i\left[\sum_{p=i}^{n}m_p\mathbf{T}_p(\mathbf{r}_p;1)\right] \tag{4}$$

Δ_i in the above equations is written as follows:[11]

$$\Delta_i=\begin{bmatrix}\lambda_i\tilde{\mathbf{z}}_{i-1} & [\lambda_i\tilde{\mathbf{p}}_{i-1}+\varphi_i\mathbf{I}]\mathbf{z}_{i-1}\\ \mathbf{0} & 0\end{bmatrix} \tag{5}$$

where $\lambda_i=1$ for revolute joints and $\lambda_i=0$ for prismatic joints, and $\varphi_i=1-\lambda_i$. $\mathbf{I}$ is a unity matrix. The symbol '~' in (5) denotes a skew symmetric matrix with zero diagonal values. For example, given a vector $\mathbf{u}=\{u_x,\ u_y,\ u_z\}^T$, $\tilde{\mathbf{u}}$ is defined as:

$$\tilde{\mathbf{u}}=\begin{bmatrix}0 & -u_z & u_y\\ u_z & 0 & -u_x\\ -u_y & u_x & 0\end{bmatrix}$$

The remaining parameters are all defined in the nomenclature.

Equations (1) to (5) are used to model the system, where $n=2$ is used for the first phase and $n=3$ is used for the second phase.

3.2. Dynamic model for the case of impact

Consider the case whereby the base is rotating about edge A (Fig. 2c). Due to the movement of the manipulator mounted on the machine, the base may reverse its direction and collide with the ground over edge B. This impact has effects on the velocities and internal forces of the manipulator. Firstly, the velocities representing joint rates change instantaneously. Secondly, large impulsive torque develops at each joint. Zheng and Hemami[10] studied the collision of a robot end-effector with the environment. Mathematical models were derived, which established quantitative relations between impulsive torques, abrupt changes in velocities and the severity of the collision. Their method has been adapted to the case in this paper.

With reference to Fig. 2c, when the base touches the ground at edge B. the contact between the base and the

https://doi.org/10.1017/S0263574701003356 Published online by Cambridge University Press

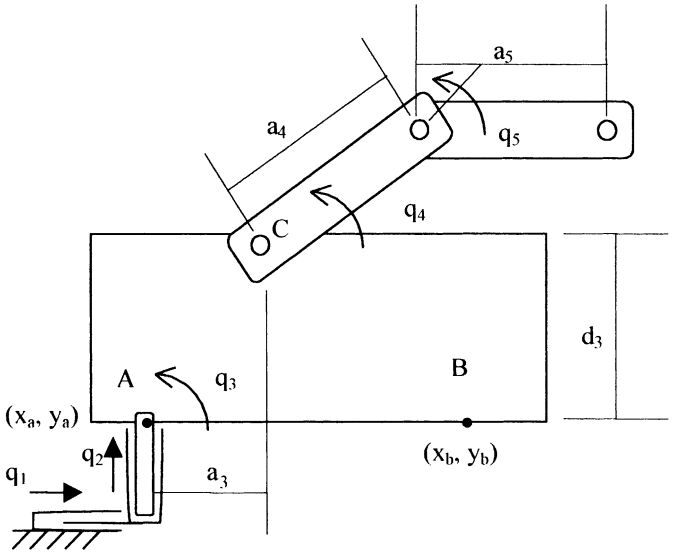

Fig. 3. Schematics of the manipulator including the virtual links.

ground at edge A is lost. Therefore, in order to establish the mathematical model during the period of collision, edge A should be considered free to translate in both horizontal and vertical directions. This means that the dynamic models derived for the cases of no impact cannot be applied to compute the instantaneous changes of the joint angular velocities at the moment when the free end of the base collides with the ground. Therefore, we first derive the dynamic equations for the general case whereby both contact edges are in the air. Joint A, on which the base was originally rotating, is modeled by adding two virtual links with prismatic joints. Figure 3 shows the schematics of the manipulator including the virtual links. The virtual links have no mass and no inertia. The advantage of this assumption is that the dynamic model can be derived as that of any serial manipulator. The manipulator configuration in this phase is, the first two joints are prismatic and the last three are revolute joints (PPRRR). The link coordinate systems for this configuration are shown in Fig. 4. The Denavit-Hartenberg link coordinate parameters are shown

Table I. Mobile Manipulator Link coordinate parameters.

Link	θ_i	d_i	a_i	α_i	Variables
1	$\pi/2$	q_1	0	$\pi/2$	q_1
2	$\pi/2$	q_2	0	$\pi/2$	q_2
2a	q_3	0	$a_f = -1$ m or $a_r = 4$ m	$-\pi/2$	q_3
3	0	$d_3 = 1.5$ m	0	$\pi/2$	–
4	q_4	0	$a_4 = 5.2$ m	0	q_4
5	q_5	0	$a_5 = 1.8$ m	0	q_5

in Table 1. Equation (1) can then be used to derive the dynamic equations for this phase with $n=5$. The first two links are the virtual links, the third one is the base, the fourth link is the boom and the fifth link is the stick. When the free end of the manipulator base comes in contact with the ground, there wil1 be an instantaneous change in the velocities. Since the other end of the base is free to move, the instantaneous changes of the velocities will also be reflected on the rotation of the base in the form of rotation about the new contact point. The instantaneous change of the speed for all degrees of freedom, $\Delta\dot{\mathbf{q}} = \dot{\mathbf{q}}_{after} - \dot{\mathbf{q}}_{before}$ ($\dot{\mathbf{q}}_{before}$ denotes the joint velocities before the impact and, $\dot{\mathbf{q}}_{after}$ is joint velocity vector after the impact), upon collision with the ground, is (see the appendix for detailed derivation):

$$\Delta\dot{\mathbf{q}} = (\mathbf{D}(\mathbf{q}))^{-1}\mathbf{J}^T(\mathbf{J}\,(\mathbf{D}(\mathbf{q}))^{-1}\mathbf{J}^T)\Delta\dot{\mathbf{x}}_b \tag{6}$$

where $\mathbf{D}(\mathbf{q})$ is defined in Section 3.1 with $n=5$. $\mathbf{J} = \dfrac{\partial \mathbf{x}_b}{\partial \mathbf{q}}$ is the Jacobean matrix relating the collision point vector $\mathbf{x}_b = [x_b, y_b]$ to the corresponding joint vector. With reference to Fig. 3, we have:

$$\begin{aligned} x_b &= q_1 + l_1 \cos(q_3) \\ y_b &= q_2 + l_1 \sin(q_3) \end{aligned} \tag{7}$$

where q_1, q_2, and q_3 are elements of the joint angle vector $\mathbf{q} = [q_1, q_2, q_3, q_4, q_5]^T$. l_1 is the distance between edges A and B. From the above relation, one can easily find the Jacobean:

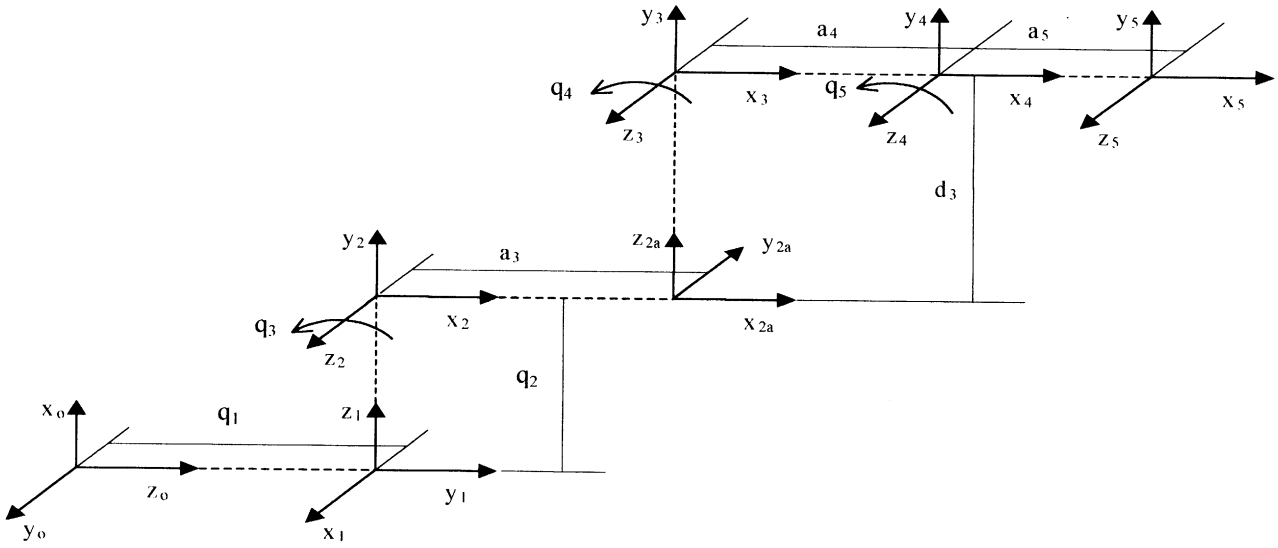

Fig. 4. Link coordinate systems pertaining to Fig. 3.

https://doi.org/10.1017/S0263574701003356 Published online by Cambridge University Press

$$\mathbf{J}=\begin{bmatrix}1 & 0 & -l_1\sin q_3 & 0 & 0\\ 0 & 1 & l_1\cos q_3 & 0 & 0\end{bmatrix} \tag{8}$$

Assuming the impact is plastic, the velocity of point B becomes zero after impact. Thus, $\Delta\dot{\mathbf{x}}_b$, the change of the velocity of the point B due to the collision with the ground, will be $\Delta\dot{\mathbf{x}}_b = -\dot{\mathbf{x}}_{b\ before}$ where $\dot{\mathbf{x}}_{b\ before}$ is the velocity of point B just before the impact. Thus

$$\dot{\mathbf{q}}_{after}=\dot{\mathbf{q}}_{before}+(\mathbf{D(q)})^{-1}\mathbf{J}^T(\mathbf{J(D(q))}^{-1}\mathbf{J}^T)(-\dot{\mathbf{x}}_{b\ before}) \tag{9}$$

Equation (9) describes the instantaneous change in the joint velocities immediately after the impact with the ground. The new joint velocities, $\dot{\mathbf{q}}_{after}$, along with current joint positions, which remain unchanged during the short duration of collision, constitute initial values of the system states for subsequent simulation times.

3.3. Modeling of the Driving Unit

Figure 5 shows the schematics of the hydraulic actuator system used in the machine under investigation. The hydraulic cylinder is connected to an open-center valve through flexible hoses. The valve monitors the flow to and from the cylinder. This system works with a constant flow pump system. With reference to Fig. 5, when the spool of the open-center valve is in neutral position, the flow passes through the valve and returns to the tank. As the spool moves to the left or to the right, the flow is distributed to the load and the tank, depending on the orifice arrangement and the load. The equations governing the flow distribution are:[12]

$$Q_i = ka_i\sqrt{P_s - P_i} \tag{10}$$

$$Q_o = ka_o\sqrt{P_o - P_e} \tag{11}$$

$$Q_e = Q - Q_i = ka_e\sqrt{P_s - P_e} \tag{12}$$

where Q_i and Q_o are the inlet and outlet flows to and from the cylinder, respectively and Q_e is the exit flow to the tank.

The rate of change of the inlet pressure $\dot{P}_i$ and the outlet pressure $\dot{P}_o$ are:

$$\dot{P}_i = \frac{\beta}{V_i(X)}(Q_i - A_i\dot{X}) \tag{13}$$

$$\dot{P}_o = \frac{\beta}{V_o(X)}(A_o\dot{X} - Q_o) \tag{14}$$

where X is the actuator displacement and $\dot{X}$ is the actuator velocity. The output force from the actuator F is

$$F = P_i A_i - P_o A_o \tag{15}$$

Finally, the torque generated by the hydraulic cylinder is

$$\tau = F\frac{dX}{dq} \tag{16}$$

where $\frac{dX}{dq}$ represents the nonlinear relationship between the actuator linear velocity and the corresponding link rotational velocity.

For the excavator under study, we have two hydraulic actuators, one for the boom and one for the stick.

4. COMPUTATIONAL ALGORITHM

During the simulation, it is important to identify different phases of the operations of the machine, i.e., whether the manipulator is going to tip over or not and if it is going to tip over about which edge it will. This is done by calculating the net moment about the front and rear edges of the base.

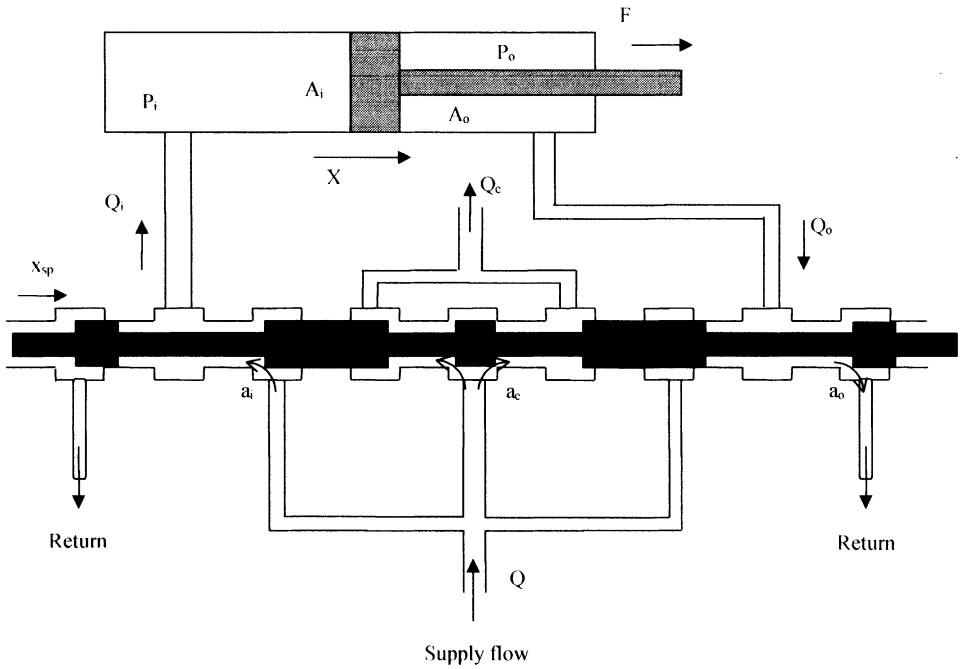

Fig. 5. Open-center valve used in mobile hydraulic manipulators.

https://doi.org/10.1017/S0263574701003356 Published online by Cambridge University Press

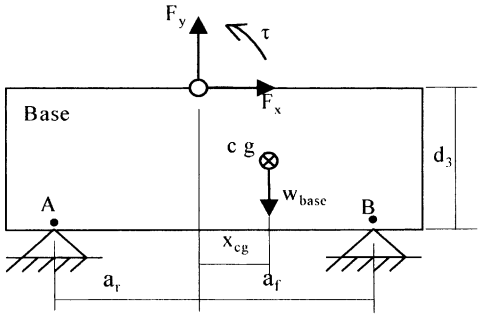

Fig. 6. Base under gravitational force and interaction forces/ torque from the manipulator.

To calculate the net moment, the interaction forces and torque between the manipulator and the base should continuously be determined. The forces and torque are shown in Fig. 6 as F_x, F_y, and τ, respectively. They are calculated using any conventional method such as Newton-Euler. The virtual link method developed by Abo-Shanab *et al.*[13] is used in this paper which is an easy and straightforward method of modeling the coupling forces for interconnected rigid bodies. Once the forces are calculated, the net moments about the rear and front edges are computed (see Fig. 6):

$$M_f = \tau + w_{base}(a_f - x_{cg}) - F_x\, d_3 - F_y\, a_f \tag{17}$$

$$M_r = \tau - w_{base}(a_r + x_{cg}) - F_x\, d_3 + F_y\, a_r \tag{18}$$

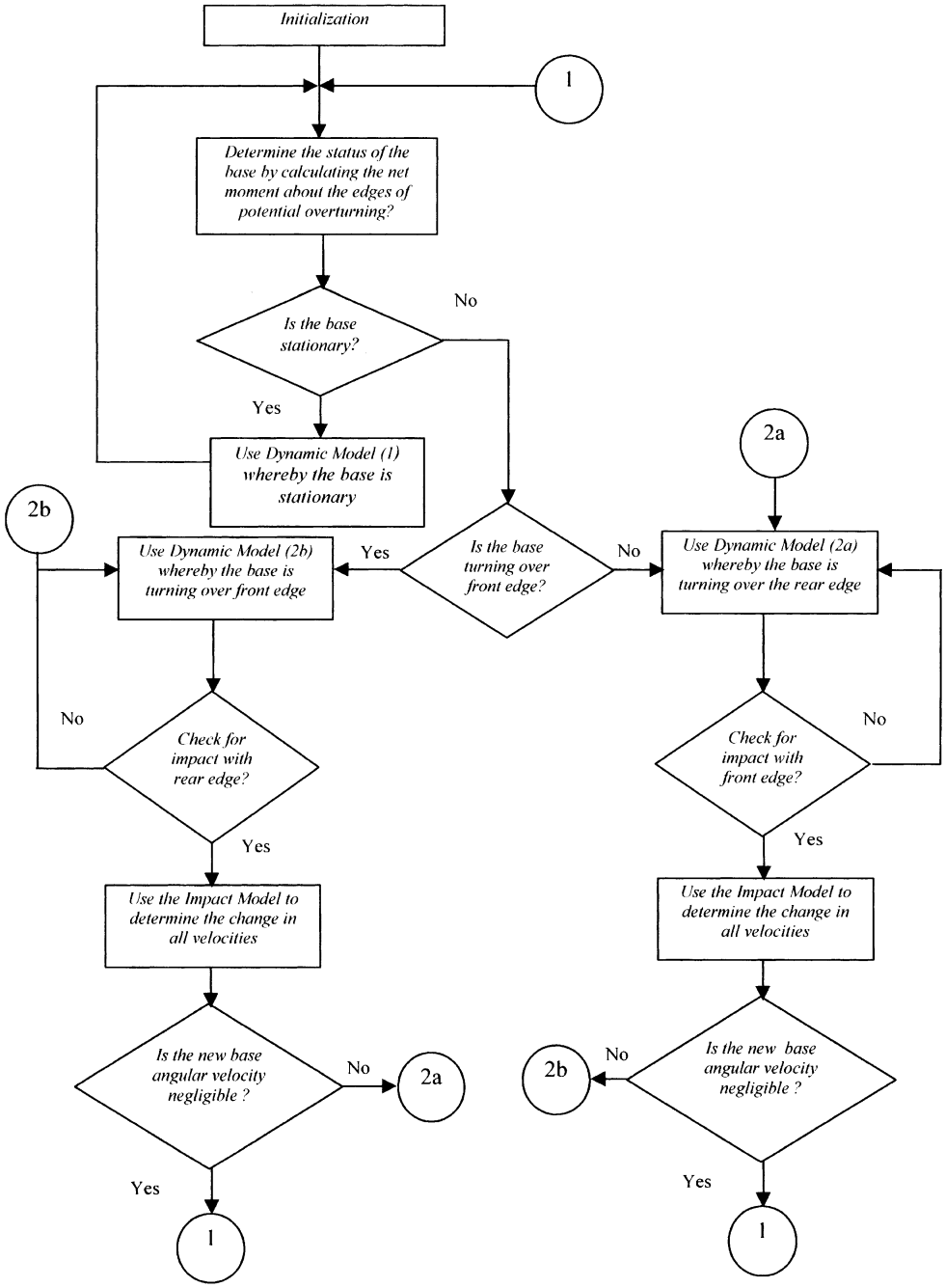

Fig. 7. Flow chart of simulation.

https://doi.org/10.1017/S0263574701003356 Published online by Cambridge University Press

Table II. Dynamic Parameters.

	Mass (kg)	Mass moment of inertia (kg m^2)	Center of gravity (x, y, z) m	Coordinate frame
base	12,000	90,523	(− 2.0, − 0.6, 0.0)	(x_3, y_3, z_3)
Boom	1,830	15,500	(− 2.9, 0.2, 0.0)	(x_4, y_4, z_4)
Stick	688	610	(− 0.9, 0.1, 0.0)	(x_5, y_5, z_5)

According to the values of M_f (net moment about the front edge) and M_r (net moment about the rear edge), one can determine about which edge the mobile manipulator is going to tip over:

$$\begin{array}{lll} M_f > 0 \text{ and } M_r < 0 & \text{the base is stationary (phase 1).} \\ M_f > 0 \text{ and } M_r > 0 & \text{the base turns over the rear edge (phase 2a).} \\ M_f < 0 \text{ and } M_r < 0 & \text{the base turns over the front edge (phase 2b).} \end{array} \quad (19)$$

Figure 7 shows the flow chart of the simulation. With reference to this figure, the computational algorithm is stated as follows:

1. Input the initial values for the joint variables, **q**, joint velocities, $\dot{\mathbf{q}}$, and the voltage signals applied to the hydraulic valves.
2. Calculate the net moments about the front and rear edges, M_f and M_r, from (17) and (18).
3. Determine the status of the manipulator, from (19);
   (i) **Phase 1**; use dynamic model ***1***, equation (1) with $n=2$, to calculate the joint variables q_4 and q_5.
   (ii) **Phase 2a**; use dynamic model ***2a***, equation (1) with $n=3$ and $a_3=a_r$ to calculate the joint variables q_3, q_4, and q_5.
   (iii) **Phase 2b**; use dynamic model ***2b***, equation (1) with $n=3$ and $a_3=-a_f$, to calculate the joint variables q_3, q_4, and q_5.
4. For cases (3ii) and (3iii), if the joint variable q_3 becomes less than a small value, ε, this means that there is an impact with the ground. So, equation (9) is used to calculate the new values of the joint velocities after the impact.
5. If the new rotational velocity of the base, $\dot{q}_3$, is negligible, then the machine is considered to be resting on both edges and the first phase of the simulation is applied. Otherwise, it will start to turn over the other edge, i.e., if the base is rotating about the front edge then, after the impact it will turn over the rear edge and *vice versa*.

5. SIMULATION RESULTS

In this section, the results of simulation studies are presented to demonstrate the usefulness of the simulation

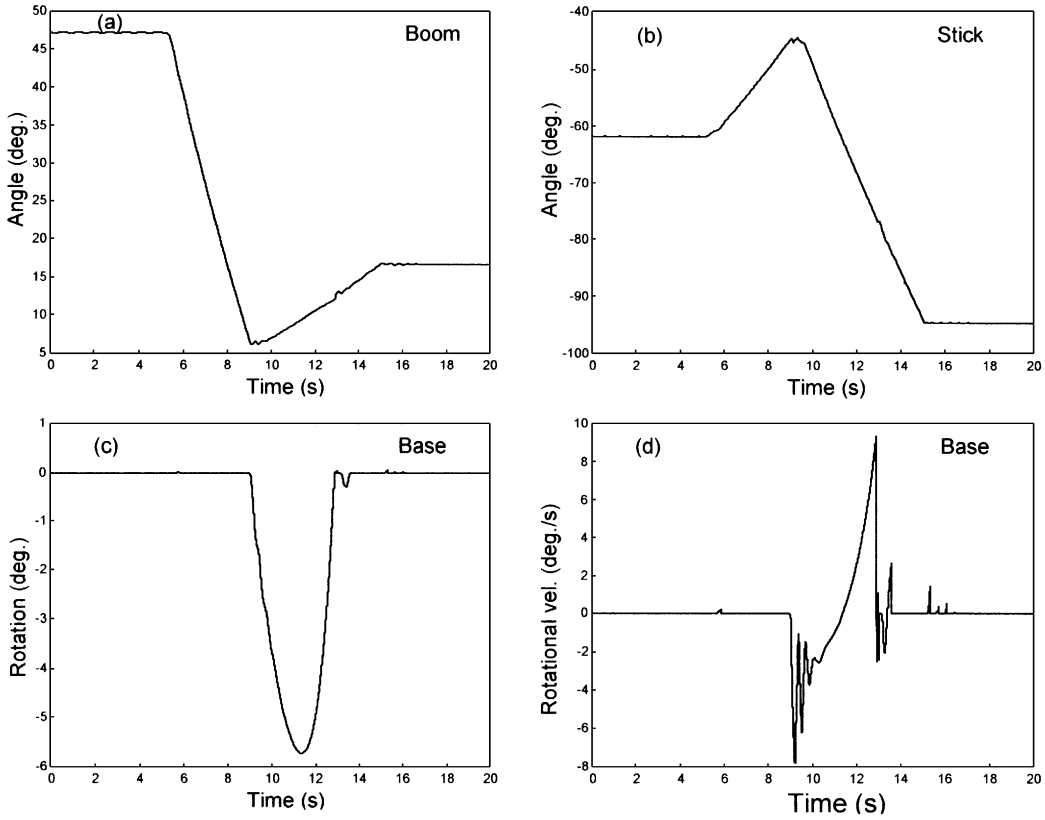

Fig. 8. Simulation results for excavator-based log-loader over a horizontal plane.

https://doi.org/10.1017/S0263574701003356 Published online by Cambridge University Press

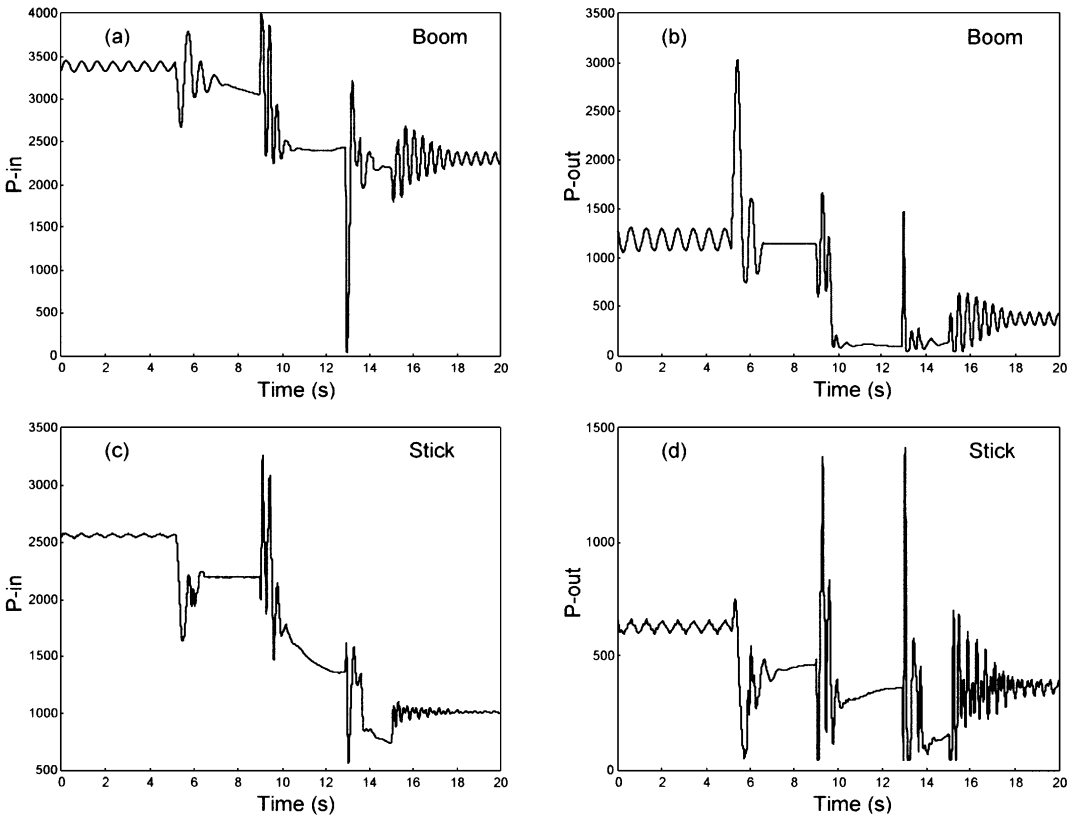

Fig. 9. Input and output line pressures.

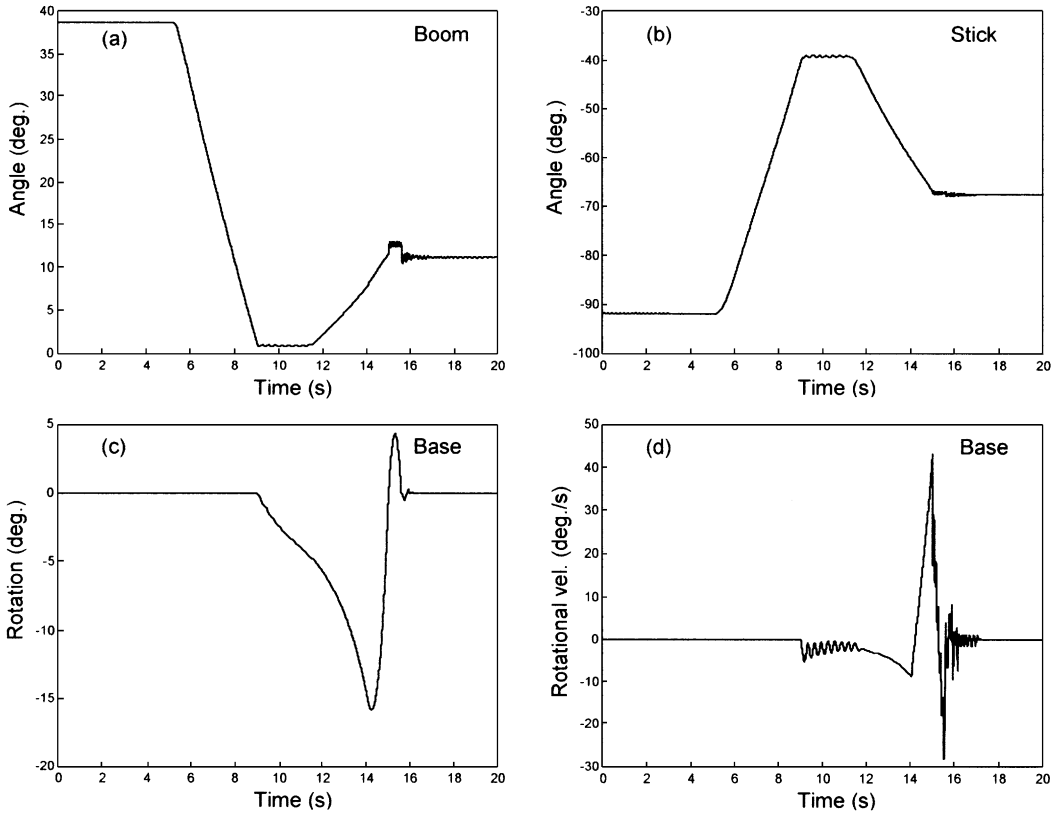

Fig. 10. Simulation results for excavator-based log-loader over an inclined plane.

https://doi.org/10.1017/S0263574701003356 Published online by Cambridge University Press

model developed here. Key system parameters are listed in Table II. Two case studies are simulated. The first case simulates a typical operation of the log-loader staying on a horizontal ground. The task is to have the machine end effector to perform a pick and place operation. In this task, the end-effector starts from a position close to the base carrying a 5000 kg load. The base is initially stable. The manipulator extends the arms to a possible 'dumping position' far from the base (see Figs. 8a and 8b). With reference to Fig. 8c, this move causes the machine to topple over. After the base rotates about 6 degrees over the front edge, the end-effector retracts back to regain the stability. As is seen, the machine starts to roll back to a stable position. Figure 9 shows the input and output line pressures for both boom and stick hydraulic actuators.

The second case describes a task whereby the machine picks up a 4000 kg load while it is on an inclined plane (-20 degrees slope). When the machine starts to lift the load, it starts to tip over. After the base rotates about 15 degrees over the front edge, the load is dropped. As shown in Fig. 10, the machine regains stability after dropping the load.

The model developed in this paper is also compared with the energy stability measure developed by Ghasempoor and Sepehri.[8] Quantitatively, the two methods give similar indication about the stability of the mobile manipulator except for the stances where the base is tipping over. The energy stability measure does not predict the states of the mobile manipulator during this period; thus, it cannot advise of any movements of the boom or the stick in order to help recover from the tipover. The present model can describe the states of the mobile manipulator during the tipover and potentially can help to recover from it. For example, the energy stability level of the manipulator has been calculated for the first case study and the result is shown in Fig. 11. Comparing Fig. 11 with Fig. 8c, the two methods give the same indication about the stability of the mobile manipulator before the tipover (time period 0 to 9 seconds), and after the tipover (time period 13.5 to 20 seconds). During the time period 9 to 13.5 seconds, where the tipover occurs, the energy stability measure calculation is not valid whereas the present method gives information about the manipulator states.

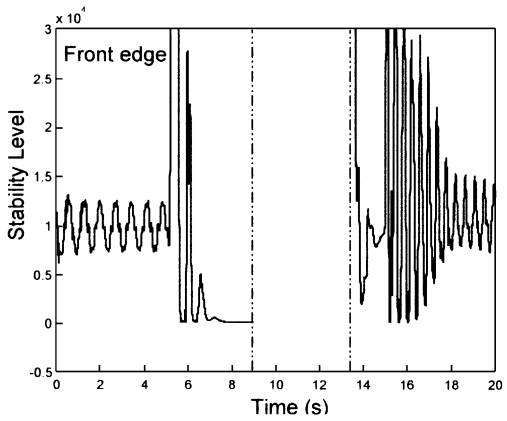

Fig. 11. Energy stability level of front edge for the case shown in Fig. 8.

6. CONCLUSION

In this paper, a dynamic model for a two-link planar manipulator mounted on a moveable platform, was developed. Building upon the model that was developed and tested in Sepehri *et al.*,[9] the current model takes into account both the hydraulic actuation function and the detailed dynamics of the base that can rock back-and-forth during the movement of the manipulator. Also, the current model takes into account the impact with the ground. Both aspects of the impact, i.e., changes in the generalized states of the system and creation of impulsive forces, are incorporated in the model. Simulation results were presented to substantiate the model development presented here. In particular, the results were found to be consistent with the ones from the previously developed energy stability method by Ghasempoor and Sepehri.[8] The energy stability method, however, does not predict how the base responds to the movement of manipulator links, whereas, the present method produces detailed behavior of the manipulator including the movement of the base.

The results of this work, which will serve as a good guide to the stability analysis of manipulators mounted on mobile platforms, clearly showed the effect of the manipulator movement on the overturning of such machines. Also, it was shown that by proper manipulation of the linkages, one can achieve a stable condition and even reverse tipover situations. This is significant, since with the introduction of computer control, safety, productivity and lifetime of mobile manipulators could be improved by automatic prediction, prevention and recovering from tipover. Currently we are investigating how to incorporate the flexibility of the contact between the ground and the base in the models developed here.

References

1. N. Sepehri, P.D. Lawrence, F. Sassan, and R. Frenette, "Resolved mode teleoperated control of Heavy Duty Hydraulic Machines," *ASME Journal of Dynamic Systems, Measurement, and Control*, **116**, 232–240 (1994).
2. D. Messuri and C. Klein, "Automatic Body Regulation for Maintaining Stability of a Legged Vehicle During Rough-Terrain Locomotion," *IEEE Journal of Robotics and Automation*, **RA-1**, No.3, 132–141 (1985).
3. S. Dubowsky and E.E. Vance, "Planning Mobile Manipulator Motions Considering Vehicle Dynamic Stability Constraints," *Proceedings IEEE International Conference on Robotics and Automation*, Scottsdale, AZ, **3**, 1271–1276 (1989).
4. S. Sugano, Q. Huang and I. Kato, "Stability criteria in controlling mobile robotic systems," *Proceedings IEEE/RSJ International Conference on Intelligent Robots and Systems*, Yokohama, **Vol. 3**, 832–836 (1993).
5. Q. Huang, S. Sugano and K. Tanie, "Motion planning for a mobile manipulator considering stability and task constraints," *Proceedings IEEE International Conference on Robotics and Automation*, Leuvan, Belgium, **Vol. 3**, 2192–2198 (1998).
6. E.G. Papadopoulos and D.A. Rey, "A new measure of tipover stability margin for mobile manipulators," *Proceedings IEEE International Conference on Robotics and Automation*, Minneapolis, Minnesota, 3111–3116 (1996).
7. D.A. Rey and E.G. Papadopoulos, "On-Line Automatic Tipover Prevention For Mobile Manipulators," *Proceedings IEEE International Conference on Intelligent Robots and Systems*, Piscataway, **Vol. 3**, 1273–1278 (1997).

https://doi.org/10.1017/S0263574701003356 Published online by Cambridge University Press

8. A. Ghasempoor and N. Sepehri, "A measure of Stability for Mobile Manipulators With Application to Heavy Duty Hydraulic Machines," *ASME Journal of Dynamic Systems, Measurement, and Control*, **Vol. 120**, 360–370 (1998).
9. N. Sepehri, F. Sassani, P.D. Lawrence and A. Ghasempoor, "Simulation and Experimental Studies of Gear Backlash and Stick-slip Friction in Hydraulic Excavator Swing Motion," *ASME Journal of Dynamic Systems, Measurement, and Control*, **118**, 463–467 (1996).
10. Y. Zheng and H. Hemami, "Mathematical Modeling of a Robot Collision with its Environment," *Robotic Systems*, **2**, 289–307 (1985).
11. M.M. Sallam, R.F. Abo-Shanab and A.A. Nasser, "Modified Methods for Dynamic Modeling of Robot Manipulators," *Proceedings ASME Design Engineering Technical Conference*, Atlanta, GA, Paper No. DETC98/MECH5860 (1998).
12. N. Sepehri and P.D. Lawrence, "Mechatronic System Techniques in Teleoperated Control of Heavy-Duty Hydraulic Machines," In: *Mechatronic Systems Techniques and Applications* (editor: C.T. Leondes), Gordon and Breach Science Publishers, Amsterdam, The Netherlands (2000) **Vol. 3**, 309–373 (2000).
13. R.F. Abo-Shanab, Q. Wu and N. Sepehri, "On Derivation of Dynamic Equations for interconnected Rigid Bodies," (to be presented at the American Control Conference, June 2001, Arlington, VA.).
14. S. Tzafestas, M. Raibert and C. Tzafestas, "Robust Sliding-Mode Control Applied to a 5-Link Biped Robot," *J. Intelligent and Robotic Systems*, **15**, 67–133 (1996).

APPENDIX

Derivation of instantaneous velocity change due to collision with the ground[10, 14]

When a manipulator comes in contact with the environment, a geometric constraint is enforced to the system motion. The result will be an impact with a sharp change of the joint velocities.[10] lt is therefore required to compute the new joint velocities just after each collision. Consider an *n*-link manipulator with the following dynamics:

$$\tau = \mathbf{D(q)}\ddot{\mathbf{q}} + \mathbf{C}(\mathbf{q}, \dot{\mathbf{q}}) + \mathbf{H(q)} \tag{A1}$$

Suppose that the end-effector of one part of the manipulator collides with the environment. The position of the contact point on this manipulator is denoted by $\mathbf{x}_b$ in the base coordinate system. $\mathbf{x}_b$ can be expressed in terms of the generalized coordinates, $\mathbf{q}$ as

$$\mathbf{x}_b = \mathbf{f(q)} \tag{A2}$$

Let the contact point of the environment be $\mathbf{x}_s$. When $\mathbf{x}_b = \mathbf{x}_s = \mathbf{f(q)}$, this means that an external constraint is applied. In association with each constraint, a generalized force Γ, acts on the system equations:

$$\Gamma = \left[\frac{\partial \mathbf{f(q)}}{\partial \mathbf{q}}\right]^T \lambda = \mathbf{J}^T\lambda \tag{A3}$$

Where $\mathbf{J}$ is the Jacobean and λ is a suitable column vector of Lagrange multipliers. Then, the equation of motion for the constraint system is:

$$\tau + \mathbf{J}^T\lambda = \mathbf{D(q)}\ddot{\mathbf{q}} + \mathbf{C}(\mathbf{q}, \dot{\mathbf{q}}) + \mathbf{H(q)} \tag{A4}$$

In the case of collision, the constraint is brought about at the moment of impact. The constraint force is subject to an abrupt change immediately after the collision. As the time of collision is infinitesimally short the constraint force can be modeled as an impulse at the moment of collision. Let the generalized constraint force vector be denoted as

$$\Gamma_\delta = \left[\frac{\partial \mathbf{f}}{\partial \mathbf{q}}\right]^T \lambda = \mathbf{J}^T\lambda$$

In the case of collision, equation (A4) becomes

$$\tau + \Gamma_\delta = \mathbf{D(q)}\ddot{\mathbf{q}} + \mathbf{C}(\mathbf{q}, \dot{\mathbf{q}}) + \mathbf{H(q)} \tag{A5}$$

During the infinitesimally short time interval of collisions, the joint positions of the system remain unchanged since joint angular velocities are finite whose integrals over an infinitesimally short time interval are zero. According to this basic assumption, one may integrate both sides of equation (A5) in an infinitesimally short time interval and have

$$\tau \lim_{\Delta t \to 0} \int_{t_O}^{t_O+\Delta t} \Gamma_\delta \quad \mathbf{dt} =$$

$$\lim_{\Delta t \to 0} \int_{t_O}^{t_O+\Delta t} \mathbf{D(q)}\ddot{\mathbf{q}}\mathbf{dt} + \lim_{\Delta t \to 0} \int_{t_O}^{t_O+\Delta t} [\mathbf{C}(\mathbf{q}, \dot{\mathbf{q}}) + \mathbf{H(q)} - \tau]\mathbf{dt} \tag{A6}$$

The second term of the left side vanishes as $\Delta t \to 0$. Equation (A6) becomes

$$\int_{t_O}^{t_O+\Delta t} \Gamma_\delta dt = \mathbf{D(q)}[\dot{\mathbf{q}}(t_o + \Delta t) - \dot{\mathbf{q}}(t_o)] \tag{A7}$$

Since the magnitude of an impulse tends towards infinite as $\Delta t \to 0$, the right side of equation (A7) converges to finite quantity. We may further denote the generalized impulsive force, $\mathbf{T}_\delta = \int_{t_o}^{t_o+\Delta t} \Gamma_\delta dt$. Then,

$$\mathbf{T}_\delta = \mathbf{J}^T \int_{t_O}^{t_O+\Delta t} \lambda dt \tag{A8}$$

From equation (A7) one may have

$$\Delta\dot{\mathbf{q}} = \dot{\mathbf{q}}(t_o + \Delta t) - \dot{\mathbf{q}}(t_o) = \mathbf{D}^{-1}(\mathbf{q})\mathbf{T}_\delta \tag{A9}$$

where $\dot{\mathbf{q}}(t_o)$ and $\dot{\mathbf{q}}(t_o + \Delta t)$ represent the joint angular velocities just before and immediately after the collision, respectively. Thus, the mathematical relation between the instantaneous change of the joint angular velocities and the generalized impulsive force is established. The relation between the change of the velocity of the point of contact on the robot and the change of the generalized angular velocity vector is:

$$\mathbf{J}[\dot{\mathbf{q}}(t_o + \Delta t) - \dot{\mathbf{q}}(t_o)] = \dot{\mathbf{x}}_b(t_o + \Delta t) - \dot{\mathbf{x}}_b(t_o) \tag{A10}$$

Using equations (A8), (A9) and (A10), we have

$$\Delta\dot{\mathbf{x}}_b = \dot{\mathbf{x}}_b(t_o + \Delta t) - \dot{\mathbf{x}}_b(t_o) = \mathbf{J}\mathbf{D}^{-1}(\mathbf{q})\mathbf{J}^T \int_{t_O}^{t_O+\Delta t} \lambda \mathbf{dt}$$

Then

$$(\mathbf{J}\mathbf{D}^{-1}(\mathbf{q})\mathbf{J}^T)^{-1}\Delta\dot{\mathbf{x}}_b = \int_{t_o}^{t_o+\Delta t} \lambda dt \tag{A11}$$

https://doi.org/10.1017/S0263574701003356 Published online by Cambridge University Press

Multiplying both sides of equation (A11) by $\mathbf{J}^T$

$$\mathbf{J}^T(\mathbf{J}\mathbf{D}^{-1}(\mathbf{q})\mathbf{J}^T)^{-1}\Delta\dot{\mathbf{x}}_b = \mathbf{J}^T\int_{t_o}^{t_o+\Delta t} \lambda dt \qquad \text{(A12)}$$

From (A8) and (A12)

$$\mathbf{T}_\delta = \mathbf{J}^T(\mathbf{J}\mathbf{D}^{-1}(\mathbf{q})\mathbf{J}^T)^{-1}\Delta\dot{\mathbf{x}}_b$$

Equation (A9) will then be

$$\Delta\dot{\mathbf{q}} = \mathbf{D}^{-1}(\mathbf{q})\mathbf{J}^T(\mathbf{J}\mathbf{D}^{-1}(\mathbf{q})\mathbf{J}^{-1}\Delta\dot{\mathbf{x}}_b \qquad \text{(A13)}$$

Equation (A13) determines the velocity change due to collision with the ground.

Nomenclature

q, $\dot{\mathbf{q}}$ and **$\ddot{\mathbf{q}}$**: vectors of the joint variables. velocities and accelerations.

$\mathbf{T}_j$: homogeneous transformation matrix from coordinate frame *i* to base coordinate frame.

$\mathbf{z}_i$: *Z*-axis of coordinate frame *i*.

$\mathbf{p}_i$: position vector of the origin of coordinate frame *i*.

$\mathbf{I}_i$: 3×3 inertial matrix of link *i* about its mass center in coordinate frame *i*.

$\mathbf{r}_i$: position vector of mass center of link *i* in coordinate frame *i*.

g: gravitational acceleration vector in base coordinate frame.

$\mathbf{x}_b$ and $\dot{\mathbf{x}}_b$: instantaneous position and velocity vectors of a robotic point coming in contact with the environment.

J: Jacobean matrix.

k: orifice coefficient.

a_i, a_o and a_e: inlet, outlet and exit areas, respectively.

P_i and P_o: input and output pressures, respectively.

P_s and P_e: supply and tank pressures, respectively.

X: actuator displacement.

$V_i(X)$ and $V_o(X)$: volumes of the fluid trapped at the sides of the actuator.

β: effective bulk modulus.

m: link mass.

https://doi.org/10.1017/S0263574701003356 Published online by Cambridge University Press